Mean-field dynamics of a Bose Josephson junction in an optical cavity

J. M. Zhang, W. M. Liu, and D. L. Zhou

Beijing National Laboratory for Condensed Matter Physics, Institute of Physics, Chinese Academy of Sciences, Beijing 100080, China

We study the mean-field dynamics of a Bose Josephson junction which is dispersively coupled to a single mode of a high-finesse optical cavity. An effective classical Hamiltonian for the Bose Josephson junction is derived, and its dynamics is studied from the perspective of a phase portrait. It is shown that the strong condensate-field interplay does alter the dynamics of the Bose Josephson junction drastically. The possibility of coherent manipulating and *in situ* observation of the dynamics of the Bose Josephson junction is discussed.

Cavity quantum electrodynamics (cavity QED) has now grown into a paradigm in the study of the matter-field interaction. To tailor the atom-field coupling effectively, a high degree of control over the center-of-mass motion of the atoms is essential. Although previous works have focused on the few-atom level [1], recently, a great step was made as two groups succeeded independently in coupling a Bose-Einstein condensate to a single-cavity mode [2,3]. That is, a single-cavity mode dressed condensate has been achieved. This opens up a new regime in both the fields of cavity QED and ultracold atom physics. In the condensate, all the atoms occupy the same motional mode and couple identically to the cavity mode, thus realizing the Dicke model [4] in a broad sense. As shown by these experiments, the condensate is quite robust; it would not be destroyed by its interaction with the cavity mode in the time scale of the experiments.

In this paper, we investigate the mean-field dynamics of a Bose Josephson junction (BJJ) [5], which is coupled to a driven cavity mode. This extends our previous work to the many-atom case [6]. The system may be constructed by splitting a Bose-Einstein condensate, which is already coupled to a single-cavity mode, into two weakly linked condensates, as can be done in a variety of ways [7–11]. We restrict ourselves to the large-detuning and low-excitation limit, so that atomic spontaneous emission can be neglected. In this limit, the effect of the strong coupling between the atoms and the field, seen by the field, is to shift the cavity resonance frequency and hence modify the field intensity. Unlike the single-condensate case, we now have two, which may couple with different strengths to the cavity mode because of the position dependence of the atom-field coupling. Consequently, the field dynamics couples to the tunneling dynamics of the BJJ and vice versa. It is the very *interplay* between the two sides that we are interested in. The interplay is made possible by the greatly enhanced atom-field coupling in a microcavity, which is unique in the context of cavity QED. In the usual optical traps and optical lattices, the interaction between the atoms and the light field is *one way* in the sense that the light field affects the motion of the atoms effectively, while the atoms have little back-action on the light field—the laser intensity is almost the same with or without the presence of the atoms. We would like to stress that, although there had already been some experimental investigations on this subject and phenomena such as dispersive optical bistability were observed [12,13], all of them dealt with thermally cold atoms. However, here, the long-range coherence of the condensates will surely make a difference.

The Hamiltonian of the system consists of three parts:

$$H = H_a + H_f + H_{\text{int}}. \tag{1}$$

H_a is the canonical Bose-Josephson-junction Hamiltonian in the two-mode approximation ($\hbar = 1$ throughout),

$$H_a = -\Omega(b_1^\dagger b_2 + b_2^\dagger b_1) + \frac{V}{2}(b_1^\dagger b_1^\dagger b_1 b_1 + b_2^\dagger b_2^\dagger b_2 b_2), \tag{2}$$

where $b_1^\dagger$, $b_2^\dagger$ (b_1, b_2) create (annihilate) an atom in its internal ground state in the left and right traps, respectively. Ω is the tunneling matrix element between the two modes, while V denotes the repulsive interaction strength between a pair of atoms in the same mode. The two-mode model assumes two stationary wave functions (the single-atom ground states actually) in the individual traps, while neglecting modifications due to the atom-atom interaction. The regime in which this approximation is valid can be found in Ref. [14]. H_f is the single-mode field Hamiltonian,

$$H_f = \omega_c a^\dagger a + \eta(t)e^{-i\omega_p t}a^\dagger + \eta^*(t)e^{i\omega_p t}a, \tag{3}$$

where ω_c and ω_p are the cavity-mode frequency and pump frequency, respectively, and $\eta(t)$, the amplitude of the pump, varies slowly in the sense that $|\dot{\eta}/\eta| \ll \omega_p$. In the limit of large detuning [15] and weak pump, the atom-field interaction is of dispersive nature, and the two-level atoms can be treated as scalar particles with the upper level being adiabatically eliminated. Under the two-mode approximation for the atoms, the interaction between the atoms and the cavity mode is [16]

$$H_{\text{int}} = U_0 a^\dagger a(J_1 n_1 + J_2 n_2), \tag{4}$$

where $U_0 = g_0^2/(\omega_c - \omega_a)$ is the light shift per photon—i.e., the potential per photon an atom feels at an antinode—g_0 being the atom-field coupling strength at an antinode. The two dimensionless parameters $J_{1,2}$ ($0 \le J_{1,2} \le 1$) measure the overlaps between the atomic modes and the cavity mode [6]. $n_1 = b_1^\dagger b_1$ ($n_2 = b_2^\dagger b_2$) counts the atoms in the left (right) trap. The term H_{int} has a simple interpretation: from the point of view of the cavity mode, its frequency is renormalized, while from the point of view of the atom ensemble, the trapping potential is tilted provided $J_1 \ne J_2$.

We would like to point out that in the interaction Hamiltonian (4), we have dropped a term $U_0 a^\dagger a J_{12}(b_1^\dagger b_2 + b_2^\dagger b_1)$, which couples the cavity mode to the atomic tunneling. Here

the dimensionless parameter J_{12} is proportional to the overlap between the two atomic modes [16] and is thus much smaller than $J_{1,2}$, which are of the order of unity. Although this type of coupling may have some nontrivial consequences [17], for our purposes we neglect it because (i) from the standpoint of the cavity mode, the atomic coherence-induced frequency renormalization is much smaller than that by the atomic densities; (ii) from the standpoint of the atoms, the cavity-induced tunneling coefficient modulation $U_0 J_{12} a^\dagger a$ is much smaller than the intrinsic tunneling coefficient Ω as long as $U_0 J_{12} \langle a^\dagger a \rangle \ll \Omega$, as is the case in the parameter regime we consider (see [28]). Technically, if this term is retained, Eqs. (9a) and (9b) below will be modified a little, and then we cannot find an effective Hamiltonian like (10) anymore. As a result, the only resource we have to analyze the behavior of the BJJ is its phase flow diagram. By numerical simulations, we do observe that modification of the phase-flow diagram of the BJJ due to the extra term is small and only quantitative.

According to the Heisenberg's equation, we have

$$i\dot{b}_1 = -\Omega b_2 + V b_1^\dagger b_1 b_1 + J_1 U_0 a^\dagger a b_1, \tag{5a}$$

$$i\dot{b}_2 = -\Omega b_1 + V b_2^\dagger b_2 b_2 + J_2 U_0 a^\dagger a b_2, \tag{5b}$$

$$i\dot{a} = [\omega_c + U_0(J_1 n_1 + J_2 n_2)]a - i\kappa a + \eta(t)e^{-i\omega_p t}. \tag{5c}$$

Note that in Eq. (5c) we have put in the term $-i\kappa a$ to model the cavity loss, with κ being the cavity-loss rate. Under the mean-field approximation, we treat the operators b_1, b_2, and a as classical quantities, $b_1 \sim \sqrt{N_1}e^{i\theta_1}$, $b_2 \sim \sqrt{N_2}e^{i\theta_2}$, and $a \sim \alpha$. Here N_1 and N_2 are, respectively, the numbers of atoms in the left and right condensates, and θ_1 and θ_2 are their phases. By taking the mean-field approximation, we are actually confined to the so-called Josephson regime as elaborated in detail in Ref. [18]. This regime is defined as $1/N \ll V/\Omega \ll N$, $N = N_1 + N_2$ being the total atom number, and is characterized by small quantum fluctuations both in the relative phase $\varphi \equiv \theta_2 - \theta_1$ ($\Delta\varphi \ll 1$) and in the populations $N_{1,2}$ ($\Delta N_{1,2} \ll \sqrt{N}$). This property then justifies the mean-field approximation. As shown in Ref. [19], the mean-field predictions (self-trapping, etc.) are well recovered in a full quantum dynamics on a short time scale, and their breakdown occurs only at a long time scale, which increases exponentially with the total atom number. We can have a glimpse of the dynamics of the system from Eq. (5). The last terms in Eqs. (5a) and (5b) reflect the fact that the BJJ is effectively tilted with an amplitude proportional to the photon number, which is a dynamical variable depending on the atom distribution of the BJJ itself, as can be seen in Eq. (5c). Consequently, we expect the BJJ dynamics to be modified, to a certain extent, by this condensate-field interplay.

It is clear from Eq. (5c) that the relaxation time scale of the cavity mode is of the order of $1/\kappa$, which is much shorter than the plasma oscillation period of a bare Bose Josephson junction [20], which, roughly speaking, is of the order of $1/\Omega$. In fact, the typical values of κ of high-finesse optical cavities are of the order of $2\pi \times 10^6$ Hz, while the experimentally observed Ω is of the order of $(2\pi \times 10)–(2\pi$

$\times 10^2$) Hz [10]. This implies that the cavity field follows the motion of the condensates adiabatically [21]; thus, from Eq. (5c) we solve

$$\langle a \rangle \equiv \alpha(t) = \frac{\eta(t)e^{-i\omega_p t}}{i\kappa + [\omega_p - \omega_c - U_0(J_1 N_1 + J_2 N_2)]} \tag{6}$$

and the photon number is

$$\langle a^\dagger a \rangle \equiv |\alpha(t)|^2 = \frac{|\eta(t)|^2}{\kappa^2 + [\Delta - \delta U_0(N_1 - N_2)/2]^2}, \tag{7}$$

where $\Delta \equiv \omega_p - \omega_c - (J_1 + J_2)NU_0/2$ and $\delta \equiv J_1 - J_2$ is the coupling difference between the two atomic modes to the cavity mode. We then see that with other parameters fixed, the photon number depends only on the atom population difference between the two traps. Moreover, the motion of the cavity mode couples to that of the condensates only in the case that the two traps are placed asymmetrically with respect to the cavity mode such that δ is nonzero. Considering that the cavity-field intensity varies rapidly along the cavity axis (with period $\lambda/2 \sim 0.5$ μm), while rather smoothly in the transverse plane (with $1/e^2$ mode waist $w \sim 10–25$ μm), and that the extension of the condensates and the separation between them are in between, it may be wise to create the coupling difference δ by a transverse rather than a longitudinal position difference between the two condensates. In the experiment of Colombe *et al.* [3], the transverse position of the cigar-shaped condensate, which is aligned parallel to the cavity axis, can be adjusted in the full range of the cavity-mode waist. On this basis, the condensate may be split along its long axis by using of the radio-frequency-induced adiabatic potential [8,9], which is also compatible with an atom chip, into two parts offset in the transverse direction. For a mode waist $w = 10$ μm, a separation $d = 1$ μm is hopeful to create a coupling difference $\delta = 0.12$ if the two condensates are located near the inflection point $x_c = w/2$ of the cavity-field intensity.

By introducing the dimensionless parameter $z = (N_1 - N_2)/N$, which describes the population of the atoms between the two traps, we rewrite the photon number (7) as

$$|\alpha(z,t)|^2 = \frac{A(t)^2}{(z - B)^2 + C^2}, \tag{8}$$

where the three dimensionless parameters are defined as $A(t) = \eta(t)/[\delta U_0 N/2]$, $B = \Delta/[\delta U_0 N/2]$, and $C = \kappa/[\delta U_0 N/2]$. We may understand $A(t)$, B, and C as the reduced pumping strength, reduced detuning, and reduced loss rate, respectively. Equation (8) implies that the photon number, as a function of z, is a Lorentzian centered at $z_c = B$ and with width $2C$. Since $-1 \leq z \leq 1$, to maximize the influence of the condensates on the cavity field, it is desirable to have B within the same interval and $C \lesssim 1$. Under these conditions, the atomic motion is able to shift the cavity in or out of resonance. Apart from the factor δ, the latter condition means that the light shift per photon times the number of atoms exceeds the resonance linewidth of the cavity, which has been realized with both a ring cavity [12] and a Fabry-Perot cavity [13].

In the following, we follow closely the line of Refs.

[22,23]. Substituting Eq. (8) into Eqs. (5a) and (5b), we find that the two equations can be rewritten in terms of z and the phase difference φ as

$$\frac{dz}{dt} = -\sqrt{1-z^2}\,\sin\phi, \tag{9a}$$

$$\frac{d\phi}{dt} = \frac{z}{\sqrt{1-z^2}}\cos\phi + rz + \frac{\delta U_0}{2\Omega}|\alpha(z,t)|^2, \tag{9b}$$

where the time has been rescaled in units of the Rabi oscillation time $1/(2\Omega)$, $2\Omega t \rightarrow t$. The dimensionless parameter $r \equiv NV/(2\Omega) > 0$ measures the interaction strength against the tunneling strength. We further define a Hamiltonian $H_c = H_c(z,\varphi,t)$ in which z and φ are two conjugate variables—i.e., $\dot{z} = -\frac{\partial H_c}{\partial \varphi}$, $\dot{\varphi} = \frac{\partial H_c}{\partial z}$. Such a Hamiltonian is

$$H_c(z,\phi,t) = -\sqrt{1-z^2}\,\cos\phi + \frac{1}{2}rz^2 + \frac{\delta U_0}{2\Omega}F(z,t), \tag{10}$$

with

$$F(z,t) = \frac{A^2(t)}{C}\arctan\left(\frac{z-B}{C}\right). \tag{11}$$

The first two terms in Eq. (10) are the Hamiltonian of a bare Bose Josephson junction as first derived in Refs. [22,23]. They describe the energy cost due to the phase twisting between the two condensates and the atom-atom repulsion, respectively. The last term may be termed as a cavity-field-induced tilt, as can be seen from its derivation. It reflects that the two traps, which are originally symmetric, are now subjected to an offset determined by the atom populations. In its nature, this term is similar to the potential an atom feels when passing a cavity adiabatically [24], with the variable z playing the role of the center of mass of the atom. The Hamiltonian can be made explicitly time dependent if the pump strength varies in time. This may offer us a tool to coherently manipulate the motion of a Bose Josephson junction [25]. However, in this work, we concentrate on the case that the pump strength is a constant, $\eta(t) \equiv \eta$, so that the system is autonomous and the Hamiltonian is conserved in time.

As a one degree-of-freedom Hamiltonian system and with the Hamiltonian itself being a first integral, the system is integrable and there is no chaos. The trajectory of the system in the phase space (plane) follows the manifold (line) of constant energy. Thus, qualitatively speaking, the dynamics of the system is to a great extent determined by the structure of its phase portrait, or more specifically, the number of stationary points, their characters (minimum, maximum, or saddle), and their locations. Before proceeding forward, we have some remarks on the structure of the phase space of the system and its implications. Superficially, the Hamiltonian H_c is defined on the rectangular domain $-1 \leq z \leq 1$, $0 \leq \varphi \leq 2\pi$. However, physically φ is periodic in 2π, and for $z = \pm 1$, φ is not well defined, so we should identify $(z,0)$ with $(z,2\pi)$ and collapse the lines $(z=\pm 1,\varphi)$ to two points [mathematically, this is justified by the fact that $H_c(z,0) = H_c(z,2\pi)$ and $H_c(1,\varphi) = C_1$, $H_c(-1,\varphi) = C_2$, with C_1, C_2 be-

ing two constants]. Therefore, the domain of the Hamiltonian or the phase space of the system is homeomorphous to a sphere. Euler's theorem for a smooth function on a sphere states that the number of minima, m_0, the number of saddles, m_1, and that of maxima, m_2, satisfy the relation $m_0 - m_1 + m_2 = 2$ [26]. This relation can be checked in Figs. 1 and 2 below.

In the following, we explore the dynamics of a Bose Josephson junction uncoupled or coupled to a cavity mode in the perspective of phase portrait. This approach has the advantage that it captures the whole information of the BJJ dynamics into one [27]. As a first step, we work out the stationary points of the system, which are determined by the equations $\frac{\partial H_c}{\partial z} = 0$, $\frac{\partial H_c}{\partial \varphi} = 0$. The second equation implies that $\varphi = 0$ or $\varphi = \pi$. Substituting these two possible values of φ into the first one, we have two equations of z, respectively,

$$f_1(z) = rz + \frac{z}{\sqrt{1-z^2}} + \frac{\widetilde{A}}{(z-B)^2 + C^2} = 0, \tag{12a}$$

$$f_2(z) = rz - \frac{z}{\sqrt{1-z^2}} + \frac{\widetilde{A}}{(z-B)^2 + C^2} = 0, \tag{12b}$$

where $\widetilde{A} = \delta U_0 A^2/(2\Omega)$. The character (minimum, saddle, or maximum) of the possible stationary points are determined by the corresponding Hessian matrices.

As a benchmark, we first consider the uncoupled case. If $r < 1$, there are a minimum $(z,\varphi) = (0,0)$ and a maximum $(z,\varphi) = (0,\pi)$. If $r > 1$, the point $(z,\varphi) = (0,0)$ remains a minimum, while $(z,\varphi) = (0,\pi)$ turns now into a saddle point, and there are two maxima at $(z,\varphi) = (\pm\sqrt{r^2-1}/r, \pi)$. The transition of the point $(z,\varphi) = (0,\pi)$ from a maximum to a saddle and the split (bifurcation) of this old maximum into two new maxima at $r = 1$ mark the onset of running-phase and π-phase self-trapping states [14,23]. Note that the aforementioned Euler's theorem carries over from $r < 1$ to $r > 1$.

For the coupled case, the roots of Eqs. (12a) and (12b) have to be solved numerically. It is natural to expect that the last term will not only shift the positions of the stationary points, but may also alter the total number of them. Thus the phase portrait of a cavity-field-coupled BJJ may be quantitatively or even qualitatively different from that of the uncoupled case. A particular example is given in Fig. 1. As shown in Figs. 1(c) and 1(d), in the specific set of parameters, both functions $f_1(z)$ and $f_2(z)$ have two new roots when the BJJ couples to the single-cavity mode. The two new roots of $f_1(z)$ give rise to a new minimum and a new saddle point along the line $\varphi = 0$, while those of $f_2(z)$ correspond to a new maximum and a new saddle point along the line $\varphi = \pi$, as clearly visible in the contour map of H_c in Fig. 1(b). Comparing Fig. 1(b) with Fig. 1(a), we see that the cavity-mode-coupled BJJ has more complex and diverse behaviors than its uncoupled counterpart. To be specific, the coupled BJJ has now three types of zero-phase modes and three types of π-phase modes, while the uncoupled BJJ possesses just one type of zero-phase mode and two types of π-phase modes. We attribute the appearance of new stationary points, and hence new motional modes of the BJJ, to the nonlinearity of
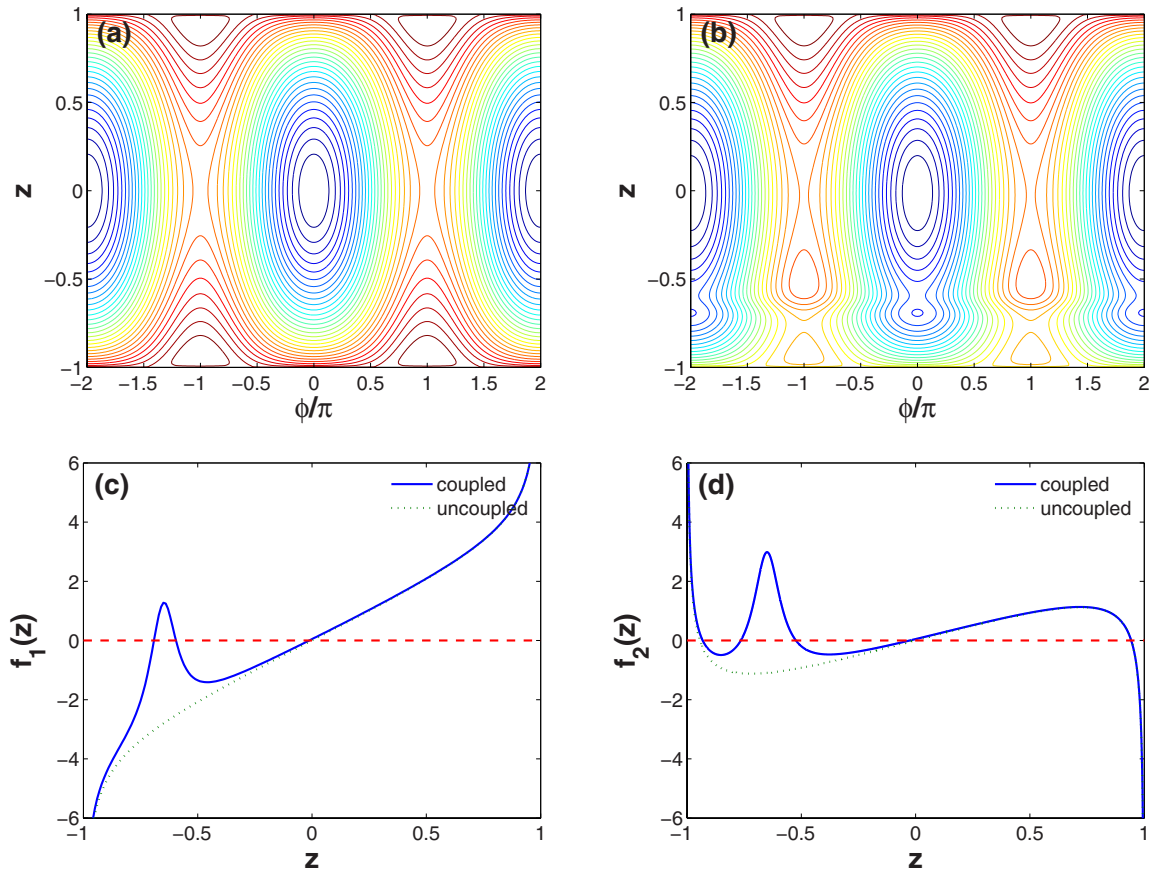
FIG. 1. (Color online) Energy contours of a Bose Josephson junction (a) uncoupled and (b) coupled to a single-cavity mode. (c) and (d) Gradient of the energy along the line $\varphi = 0$ and $\varphi = \pi$, respectively. Zeros of $f_1(z)$ with positive (negative) derivatives correspond to minima (saddle points) of H_c, while zeros of $f_2(z)$ with positive (negative) derivatives correspond to saddle points (maxima). The parameters are $NV/(2\Omega) \equiv r = 3$, $\widetilde{A} = 0.02$, $B = -0.65$, and $C = 0.07$ [28].

the cavity-field-induced tilt. To appreciate this point, let us consider the tilt due to the zero-point energy difference of the two traps or height difference in the gravitational field. That will contribute a term linear in z to the Hamiltonian H_c [22,23] and, in turn, a constant to the functions $f_{1,2}$. As a constant just shifts the graph of a function up or down as a whole, it is ready to convince oneself that no new roots will arise.
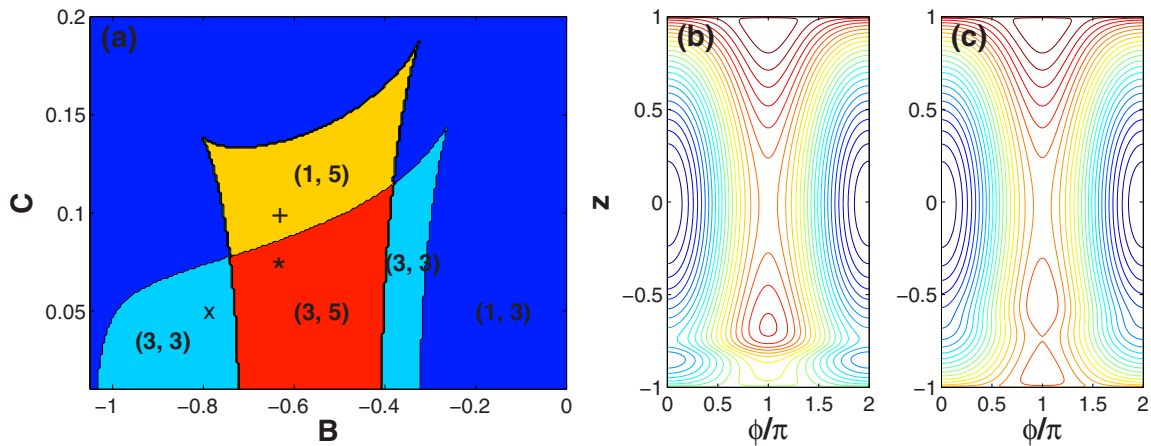

FIG. 2. (Color online) (a) A slice of the phase diagram of the Bose Josephson junction. Different regimes are differentiated by their colors and are labeled with the numbers of zeros (z_1, z_2) of the functions f_1 and f_2. The fixed parameters are $r = 3$ and $\widetilde{A} = 0.02$. The asterisk corresponds to the set of parameters in Fig. 1, while the cross and plus signs correspond to $(B, C) = (-0.8, 0.05)$ and $(B, C) = (-0.65, 0.1)$, respectively. (b) and (c) Energy contours of the Bose Josephson junction with the parameters indicated by the cross and plus signs in (a), respectively.
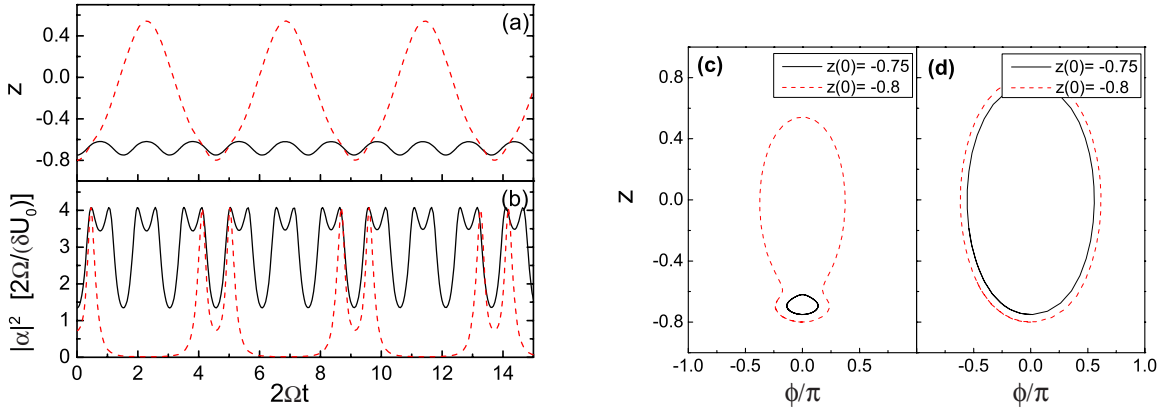
FIG. 3. (Color online) Motion of the Bose Josephson junction. (a) Atom population imbalance z and (b) intra cavity photon number $|\alpha|^2$ [in units of $2\Omega/(\delta U_0)$] versus the reduced time $2\Omega t$. The initial conditions are $(\varphi(0), z(0)) = (0, -0.75)$ (black solid lines) and $(\varphi(0), z(0)) = (0, -0.8)$ (red dashed lines). (c) and (d) Trajectories of the Bose Josephson junction (c) coupled or (d) uncoupled to the cavity mode, with the two different initial conditions above. The same parameters as in Fig. 1.

It is natural to expect that there are many other qualitatively different possibilities than the one presented in Fig. 1(b), since there are at least four free parameters in H_c. To get a general picture of this point, we present something like a phase diagram of the BJJ in Fig. 2(a). We classify the regimes according to the numbers of zeros (z_1, z_2) of the two functions $f_{1,2}$. In different regimes, the numbers of stationary points differ, and that will result in qualitatively different behaviors of the BJJ. The phase diagram strongly indicates that the BJJ dynamics can be very diverse. The (1,3) regime occurs also for a bare BJJ, as in Fig. 1(a), while the other regimes are unique to the cavity-mode-dressed BJJ. Note that these regimes are in accord with our estimation that for the condensate-field interplay to manifest itself, it is desirable to have $|B| \lesssim 1$ and $C \lesssim 1$. Figure 1(b) (indicated by the asterisk) falls in the (3,5) regime, and two representative cases (indicated by the cross and plus signs, respectively) in the (3,3) and (1,5) regimes are given in Figs. 2(b) and 2(c).

We note that the cavity mode plays a *dual* role here. On the one hand, it plays with the condensates interactively and modifies their dynamics effectively; on the other hand, it also carries with it information on the population of the atoms between the two traps as it leaks out of the cavity. In Figs. 3(a) and 3(b), we plot the time evolution of the population imbalance and the number of intra cavity photons (which is proportional to the cavity output), with the latter calculated from the former by using Eq. (8). Initially, the phase $\varphi(0) = 0$ and $z(0) = -0.75$ or -0.8, respectively. Despite the minimal difference between the two initial states, the subsequent dynamics is quite different. The outputs of the cavity differ not only in their periods, but also in their detailed temporal structures. The trajectories of the BJJ, as can be read off from Fig. 1(b), are shown in Fig. 3(c). The influence of the cavity field on the BJJ dynamics can be seen by comparing Fig. 3(c) with Fig. 3(d). It is worth noting that this influence may occur at an extremely low intra cavity photon number [13,28]. If the parameters can be determined independently, we may infer the population imbalance evolution from the outputs of the cavity. This may serve as a different approach, which is nondestructive, than the usual absorption image method, to track the tunneling dynamics of two weakly linked Bose-Einstein condensates. Of course, because the atom-field interaction involves only the atom numbers [see Eq. (4) or Eqs. (6) and (7)], no information on the relative phase of the two condensates is contained in the cavity outputs. To fully characterize the dynamics of a BJJ, techniques such as the release-and-interfere technique [9–11] are still needed.

So far, our discussion has been facilitated by the two-mode approximation for atomic motion. We assumed two rigid atomic modes defined by the double-well potential. However, the interaction with the cavity mode provides a time-varying optical lattice potential for the atoms, and that may disturb the atomic modes chosen *a priori*. We then need to check the validity of the two-mode approximation for consistency. For a cigar-shaped condensate with a length much larger than the cavity-mode wavelength λ, the long-range coherence of the condensate and the uncertainty relation imply that the atomic axial momentum distribution is localized around $p = 0\hbar k$ with a width much smaller than $\hbar k$ ($k = 2\pi/\lambda$) [29]. The intra cavity optical lattice potential couples the $p = 0\hbar k$ atomic mode to the $p = \pm 2\hbar k$ modes. The coupling strength is approximately $|\alpha|^2 U_0/2$, and the energy gap between the two manifolds is about 4 times the recoil energy of the atoms. Here the former is on the order of $2\pi \times 1$ kHz [28], while the latter is about $4E_r = 2\pi \times 100$ kHz (for ^{23}Na). Thus the intracavity optical lattice can be considered as a weak perturbation and the contamination of higher-momentum modes in the condensate wave function is negligible. Therefore, it is safe to take the two-mode approximation under some circumstances. Of course, the two-mode approximation is just technical; the interplay between the condensate and the cavity field does not depend on it. Even if in the future we have to go beyond the two-mode approximation, we believe the interplay is still there.

Another possible detrimental effect the cavity may introduce is to heat up the condensate, because of the temporal fluctuations of the intracavity photon number and hence the fluctuations of the optical lattice [30]. That may give rise to atom loss and may damp the Josephson oscillation, and it deserves further study.

In conclusion, we have derived an effective Hamiltonian

for a Bose Josephson junction dispersively coupled to a single-cavity mode under the mean-field approximation. The dynamics of the Bose Josephson junction was studied by means of phase portraits, and we found that it can be substantially different from that of a bare Bose Josephson junction, due to the strong condensate-field interplay. Moreover, the dynamics of the cavity-mode-coupled Bose Josephson junction is very diverse. By engineering the parameters, a large variety of possibilities are accessible, as shown in Fig. 2. Although in this work, as a starting point, we have restricted ourselves to the time-independent case, it may be interesting to go into the time-dependent case. By using an external feedback depending on the outputs of the cavity [31], *in situ* observation and manipulation of the state of a Bose Josephson junction may be possible. Furthermore, generalization of the present scenario to a Josephson junction array [32] may be worth consideration. That will allow us to study the cavity-mediated long-range interactions [33] between far-separated condensates.

[1] K. M. Fortier, S. Y. Kim, M. J. Gibbons, P. Ahmadi, and M. S. Chapman, Phys. Rev. Lett. **98**, 233601 (2007); A. D. Boozer, A. Boca, R. Miller, T. E. Northup, and H. J. Kimble, *ibid.* **97**, 083602 (2006); S. Nußmann, M. Hijlkema, B. Weber, F. Rohde, G. Rempe, and A. Kuhn, *ibid.* **95**, 173602 (2005).

[2] F. Brennecke, T. Donner, S. Ritter, T. Bourdel, M. Köhl, and T. Esslinger, Nature (London) **450**, 268 (2007).

[3] Y. Colombe, T. Steinmetz, G. Dubois, F. Linke, D. Hunger, and J. Reichel, Nature (London) **450**, 272 (2007).

[4] R. H. Dicke, Phys. Rev. **93**, 99 (1954).

[5] For some topical reviews, see R. Gati and M. K. Oberthaler, J. Phys. B **40**, R61 (2007); and also F. Sols, in *Bose-Einstein Condensation in Atomic Gases*, Proceedings of the International School of Physics "Enrico Fermi," Course CXL, edited by M. Inguscio, S. Stringari, and C. Wieman (IOS Press, Amsterdam, 1999).

[6] J. M. Zhang, W. M. Liu, and D. L. Zhou, Phys. Rev. A **77**, 033620 (2008).

[7] S. Levy, E. Lahoud, I. Shomroni, and J. Steinhauer, Nature (London) **449**, 579 (2007).

[8] S. Hofferberth, I. Lesanovsky, B. Fischer, J. Verdu, and J. Schmiedmayer, Nat. Phys. **2**, 710 (2006).

[9] T. Schumm, S. Hofferberth, L. M. Andersson, S. Wildermuth, S. Groth, I. Bar-Joseph, J. Schmiedmayer, and P. Krüger, Nat. Phys. **1**, 57 (2005).

[10] M. Albiez, R. Gati, J. Folling, S. Hunsmann, M. Cristiani, and M. K. Oberthaler, Phys. Rev. Lett. **95**, 010402 (2005).

[11] Y. Shin, M. Saba, T. A. Pasquini, W. Ketterle, D. E. Pritchard, and A. E. Leanhardt, Phys. Rev. Lett. **92**, 050405 (2004).

[12] J. Klinner, M. Lindholdt, B. Nagorny, and A. Hemmerich, Phys. Rev. Lett. **96**, 023002 (2006); Th. Elsässer, B. Nagorny, and A. Hemmerich, Phys. Rev. A **69**, 033403 (2004); B. Nagorny, Th. Elsässer, and A. Hemmerich, Phys. Rev. Lett. **91**, 153003 (2003).

[13] S. Gupta, K. L. Moore, K. W. Murch, and D. M. Stamper-Kurn, Phys. Rev. Lett. **99**, 213601 (2007).

[14] G. J. Milburn, J. Corney, E. M. Wright, and D. F. Walls, Phys. Rev. A **55**, 4318 (1997).

[15] In contrast to the single-atom case, here we have to take into account the collective behavior of the atoms. Thus the large detuning condition corresponds to $|\omega_c - \omega_a| \geqslant g_N = g_0 \sqrt{J_1 N_1 + J_2 N_2}$ for all relevant pairs (N_1, N_2); see also the supplementary information of Ref. [3].

[16] I. B. Mekhov, C. Maschler, and H. Ritsch, Phys. Rev. A **76**, 053618 (2007); Nat. Phys. **3**, 319 (2007); C. Maschler and H. Ritsch, Phys. Rev. Lett. **95**, 260401 (2005).

[17] J. Ye (private communication).

[18] A. J. Leggett, Rev. Mod. Phys. **73**, 307 (2001); G. S. Paraoanu, S. Kohler, F. Sols, and A. J. Leggett, J. Phys. B **34**, 4689 (2001).

[19] S. Raghavan, A. Smerzi, and V. M. Kenkre, Phys. Rev. A **60**, R1787 (1999).

[20] Its cavity-mode-coupled counterpart may be referred to as a cavity-mode-"dressed" Bose Josephson junction; see also the concept of "dressed Bose-Einstein condensates" in E. V. Goldstein, E. M. Wright, and P. Meystre, Phys. Rev. A **57**, 1223 (1998).

[21] P. Horak, S. M. Barnett, and H. Ritsch, Phys. Rev. A **61**, 033609 (2000).

[22] A. Smerzi, S. Fantoni, S. Giovanazzi, and S. R. Shenoy, Phys. Rev. Lett. **79**, 4950 (1997).

[23] S. Raghavan, A. Smerzi, S. Fantoni, and S. R. Shenoy, Phys. Rev. A **59**, 620 (1999).

[24] S. Haroche, M. Brune, and J. M. Raimond, Europhys. Lett. **14**, 19 (1991).

[25] M. S. Chang, Q. Qin, W. Zhang, L. You, and M. S. Chapman, Nat. Phys. **1**, 111 (2005).

[26] V. I. Arnold, *Ordinary Differential Equations* (MIT Press, Cambridge, MA, 1973), p. 262.

[27] P. Buonsante, R. Franzosi, and V. Penna, Phys. Rev. Lett. **90**, 050404 (2003).

[28] We think this set of parameters is experimentally practical. By taking $2\Omega \sim 2\pi \times 10^2$ Hz, $\kappa \sim 2\pi \times 10^6$ Hz, $U_0 \sim 2\pi \times 10^4$ Hz, $\delta \sim 0.1$, $J_{12} \sim 0.01$, $r \sim 10$, $N \sim 10^4$, and $A \sim 10^{-2}$, we have $\tilde{A} \sim 0.01$, $C \sim 0.1$, and $|\alpha|^2 \sim 0.01$. Note that B is free by adjusting the cavity pump detuning.

[29] J. Stenger, S. Inouye, A. P. Chikkatur, D. M. Stamper-Kurn, D. E. Pritchard, and W. Ketterle, Phys. Rev. Lett. **82**, 4569 (1999).

[30] K. W. Murch, K. L. Moore, S. Gupta, and D. M. Stamper-Kurn, Nat. Phys. **4**, 561 (2008).

[31] P. W. H. Pinkse, T. Fischer, P. Maunz, and G. Rempe, Nature (London) **404**, 365 (2000); C. J. Hood, T. W. Lynn, A. C. Doherty, A. S. Parkins, and H. J. Kimble, Science **287**, 1447 (2000).

[32] G. S. Paraoanu, Phys. Rev. A **67**, 023607 (2003).

[33] P. Münstermann, T. Fischer, P. Maunz, P. W. H. Pinkse, and G. Rempe, Phys. Rev. Lett. **84**, 4068 (2000).